The ATHENA Antihydrogen Experiment

K.S. Fine (for the ATHENA Collaboration*)

CERN-CH, Division EP, 1211 Geneva 23, Switzerland

Abstract. The ATHENA experiment is being built at CERN to produce and trap neutral antihydrogen. Here we give an overview of the plans to produce antihydrogen. The experiment must 1) trap the antiprotons produced by the CERN accelerators, 2) produce and trap positrons, 3) combine the two charge species into antihydrogen, and finally 4) detect the presence of the antihydrogen. In this paper we discuss how we intend to accomplish each of these steps.

INTRODUCTION

The ATHENA experiment is being constructed at CERN with the goal of producing neutral antihydrogen ($\overline{\mathrm{H}}$) for precise laser spectroscopy. A second experiment at CERN with a similar goal is being built by the ATRAP collaboration (1). The most important scientific goals are to test CPT invariance and to measure the gravitational charge of antimatter (2). This paper focuses on the plans for the production of antihydrogen.

Producing $\overline{\mathrm{H}}$ involves several steps: 1) trap and cool $\overline{\mathrm{p}}$'s made by the CERN accelerators, 2) produce and trap an e^+ plasma and 3) combine the two to form $\overline{\mathrm{H}}$. Finally, the presence of $\overline{\mathrm{H}}$ must be detected. Figure 1 shows an overview of the ATHENA apparatus, designed to accomplish these goals. Antiprotons delivered by the Antiproton Decelerator (AD) arrive from the left. They enter into a superconducting magnet with a 3 Tesla field, where they are trapped in a Malmberg-Penning trap with a hyperbolic trap in the center. There they are cooled by collisions with a cold electron cloud. The electrons are cooled by emitting cyclotron radiation to the environment.

The positrons arrive from the right, generated by a ^{22}Na source. They are accumulated in a positron accumulator over a period of several minutes, then transferred to the superconducting magnet where they are also cooled by cyclotron radiation. At this point the electrons can be ejected, and then the antiprotons brought

---

* Amsler C., Bollen G., Cantone A., Carlberg C.B., Cesar C.L., Charlton M., Collier M.J.T., Doser M., Eades J., Ekloew N.A., Fedele R., Fine K.S., Fontana A., Fritioff T., Gemme G., Gorini G., Hangst J.S., Hayano R., Hermes E., Holzscheiter M.H., Jørgensen L.V., Kleppner D., Lagomarsino V., Landua R., Lewis R.A., Lodi-Rizzini E., Macrì M., Manuzio G., Marchesotti M., Merrison J.P., Pruys H., Regenfus C., Riedler P., Rotondi A., Rouleau G., Salvini P., Schuch R.H., Smith G.A., Testera G., Torelli G., Uggerhøj E., Van der Werf D. P., Venturelli L., Yamazaki T., Yamazaki Y., Zanello D., Zwahlen M.

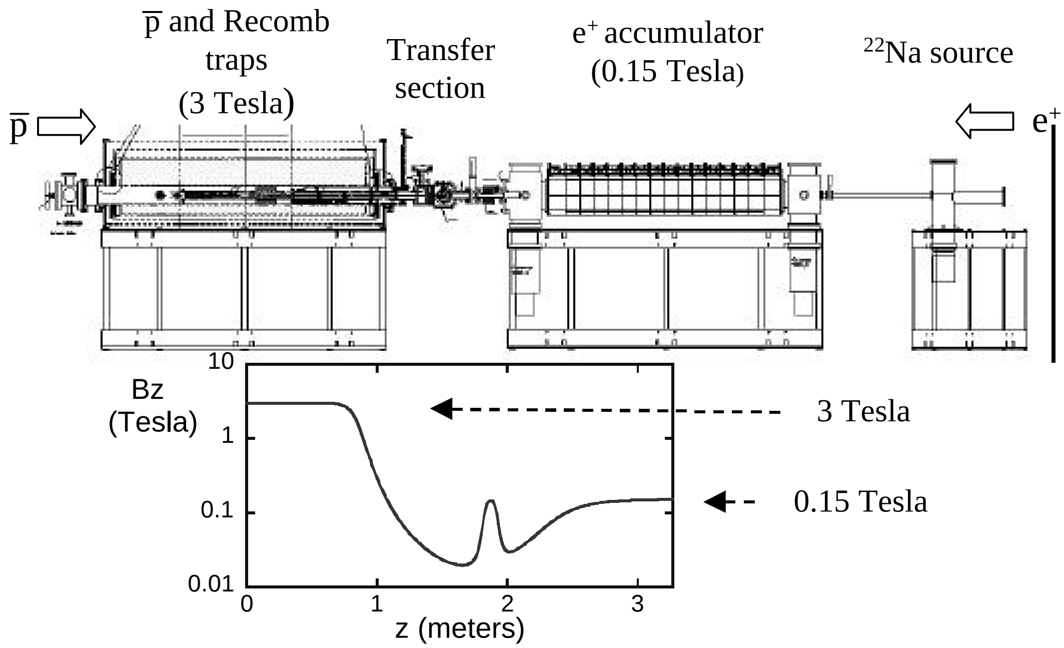

FIGURE 1: Overview of the ATHENA apparatus. Drawing is to scale; dimensions are shown on the plot of axial magnetic field at the bottom.

into contact with the positrons, where they will recombine by either two-body or three-body processes. An imaging detector surrounding the recombination trap detects the annihilations of the antihydrogen. In the following sections we will elaborate on these steps.

PRODUCTION OF ANTIPROTONS IN THE AD

Antiprotons are produced and accumulated in the Antiproton Decelerator (AD) at CERN. The antiprotons are created by colliding a 26 GeV/c proton beam with an iridium target, and then separated from other particles using a mass spectrometer. The antiprotons are then steered into the AD storage ring where they are decelerated and cooled by stochastic and electron cooling. The AD ring is capable of delivering one bunch of about 10^7 $\bar{p}$'s at a kinetic energy of 5 MeV every 2 minutes.

The AD ring is approximately 60 meters in diameter, and the antiproton experiments are installed inside this ring. There are three experiments: ASACUSA, designed to study various aspects of antiproton physics, including the spectroscopy of antiprotonic helium, the ATRAP experiment, which has already been mentioned, and the ATHENA experiment discussed in this paper. Each $\bar{p}$ bunch will be delivered to one experiment at a time.

Commissioning of the AD ring is currently foreseen to finish in November 1999. Since the CERN accelerator complex is closed during the months from December to April, the beginning of physics in the AD is expected to be in May 2000.

TRAPPING OF ANTIPROTONS

Figure 2 shows the scheme to be used to degrade and capture the antiprotons. The $\bar{p}$ bunch from the AD beam line is shown arriving from the left, where the bunch exits the AD vacuum system through a thin titanium foil. The $\bar{p}$'s make a short journey in air, where a silicon counter will be placed. The counter will be useful to trigger the voltages that trap the $\bar{p}$'s. The $\bar{p}$ beam then enters the ATHENA vacuum system through another thin titanium foil. The beam next encounters a segmented silicon detector, as shown in Fig. 2. The segments will give information about the centering and radial profile of the bunch. Note that the vacuum system shown on the right side of Fig. 2 is the bore of the 3 Tesla superconducting magnet. As the bunch enters into the bore and traverses the second silicon detector, it is compressed by the 3 Tesla magnetic field.

Inside the bore of the superconducting magnet is a second vacuum system, called the “cold nose”. This design was driven by the need to have two temperatures available: the particle traps should be at LHe temperature (4 K) to cool the particles as much as possible, while the $\bar{H}$ detector electronics operates better at LN_2 temperature (77 K). The magnet bore will be connected to the magnet LN_2 reservoir, and the detector will be thermally anchored to the bore. The cold nose will be inside the

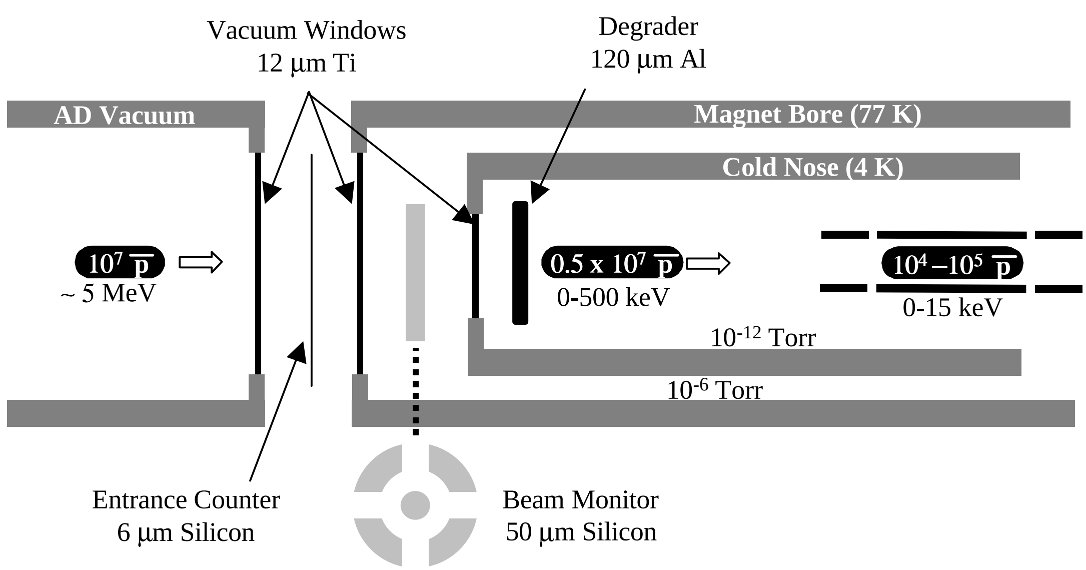

FIGURE 2: Path of the antiproton bunch into the ATHENA apparatus. The AD vacuum system is on the left, on the right is the bore of the ATHENA superconducting magnet at 10^{-6} Torr. Inside this bore is another vacuum system at 10^{-12} Torr. A very low pressure is necessary to reduce annihilation of the antiparticles by neutral atoms.

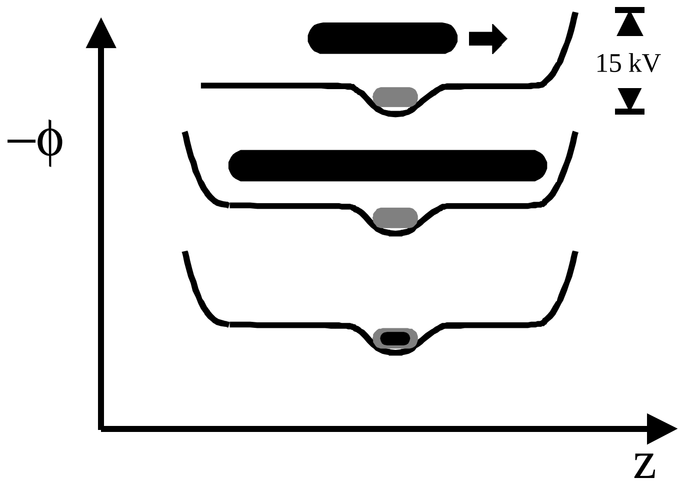

FIGURE 3: Antiproton bunch (black) is captured by quickly ramping a -15 kV potential after the $\bar{p}$ bunch enters the trap. Electron cloud (grey) is cooled by radiating cyclotron radiation, and the cold electrons cool the antiprotons by collisions.

detector, and will be cooled by a separate external cryostat. The cold nose will contain the particle traps.

Finally, the $\bar{p}$ bunch will traverse an aluminum degrader. The thickness has been chosen so that about half of the $\bar{p}$'s will annihilate, and those that emerge will be spread over the energy range from 0 to 500 keV. Those in the range from 0 to 15 keV will be trapped downstream from the degrader using the technique illustrated in Fig. 3. A cylindrical Malmberg-Penning trap will have the far end electrode at -15 kV, and will quickly ramp (~100 ns) the other end electrode to -15 kV after the $\bar{p}$ bunch enters, trapping all $\bar{p}$'s in this energy range. This will trap between 10^4 to 10^5 $\bar{p}$'s. The $\bar{p}$ cloud will then be cooled by collisions with an electron plasma trapped in a hyperbolic region of the larger trap. The electrons are cooled by cyclotron radiation (τ~0.4 sec), unlike the $\bar{p}$'s which are too massive for significant radiative cooling. Once the particles are cooled, the end potentials can be reduced to voltages below 100 volts, and the electron cloud can be ejected by quickly lowering and raising an end electrode. The light electrons will be ejected before the heavier $\bar{p}$'s can escape the trap.

PRODUCTION AND ACCUMULATION OF POSITRONS

A separate paper in this volume describes the positron accumulation scheme (3), originally developed by Cliff Surko's group at UC San Diego (4). We use the radioactive decay of ^{22}Na as an e^+ source along with a neon moderator to reduce the energy of the positrons. The positrons then fall into a Malmberg-Penning trap by

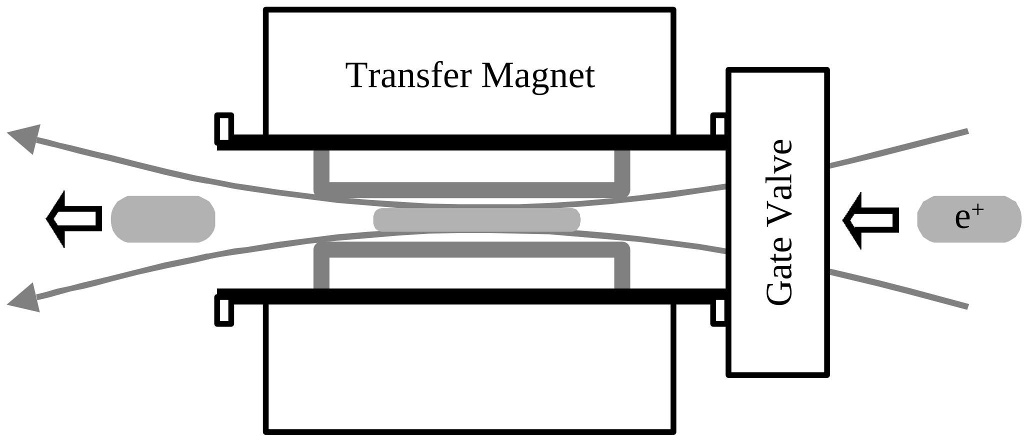

FIGURE 4: Positron transfer section. During the transfer, the radial size of the positron cloud is reduced due to the magnetic field of the transfer magnet, while the neutral buffer gas from the accumulation section is impeded by the small vacuum conductance of the tube.

losing energy due to collisions with a background N_2 buffer gas. The trap is within a normally conducting, 0.15 Tesla magnet.

Once sufficient numbers of positrons are accumulated (more than 10^8 after ~5 minutes), the pressure is reduced, and the positrons transferred to the same superconducting magnet where the antiprotons are stored. The advantage of this technique is that large numbers of positrons can be quickly accumulated. The disadvantage is that the buffer gas can leak into the antiproton trap and raise the pressure, leading to a limited lifetime of the antiprotons due to annihilation. In order to reduce the leakage of the buffer gas into the antiproton trap, a differential vacuum transfer section is being constructed.

The design of this transfer section is illustrated in Fig. 4. A vacuum gate valve will normally separate the positron accumulator from the recombination and antiproton traps, which are contained in the superconducting magnet. During the positron transfer, the gate valve is opened for a few seconds. The positrons are accelerated into the transfer section. There they are squeezed by the field of the transfer magnet to a diameter of less than 2 cm, allowing them to pass through a small electrode that will act as a “choke” for the buffer gas. This setup will maintain a pressure difference of at least a factor of 100 between the two regions.

RECOMBINATION

Once both the antiprotons and the positrons are inside the superconducting magnet and are cold, the two charge clouds must be overlapped for recombination to occur. Several schemes have been discussed to accomplish this in Malmberg-Penning traps (5).

When the two charge species are in contact, they can recombine by two-body or three body collisions (6). (There are also ideas to induce recombination with resonant laser stimulation (7)). The recombination rate scales with positron temperature T and density n as

$$\begin{aligned} &2-\text{body}: \qquad e^+ + \bar{p} \Rightarrow \bar{H} + h\upsilon \qquad R \sim n \; T^{-1/2} \\ &3-\text{body}: \quad e^+ + e^+ + \bar{p} \Rightarrow \bar{H} + e^+ \qquad R \sim n^2 \; T^{-9/2}. \end{aligned}$$

In both cases a low positron temperature and a high positron density results in a higher recombination rate. It is certain to be advantageous for the positrons to be as cold and dense as possible. This means that the best recombination rates are achieved when the positrons are in the plasma regime, *i.e.* when the Debye length $\lambda_D \equiv \sqrt{T/4\pi\, ne^2}$ becomes smaller than the size of the positron cloud (8).

The plasma temperature may be significantly higher than the electrode wall temperature (9), contrary to common belief. The electrostatic energy of a nonneutral plasma is large compared to its thermal energy, and any slow expansion of the plasma liberates electrostatic energy, which will be converted to thermal energy. Assuming collisions with neutrals can be neglected, the only cooling mechanism is cyclotron radiation. If the plasma has a radial expansion time given by τ_m, a cyclotron cooling time given by τ_c and the electric potential at the center of the plasma is ϕ_p, then in equilibrium

$$\frac{dT}{dt} \approx \frac{Ne\phi_p}{\tau_m} - \frac{NkT}{\tau_C} = 0\,,$$

where N is the number of charges in the trap. Therefore, the plasma temperature will have a lower limit of $kT/e \approx (\tau_c/\tau_m)\,\phi_p$. At the 3 Tesla field planned for ATHENA, τ_c~0.4 seconds. If the potential of the positron cloud is 10 Volts, this requires expansion times $\geq 10^4$ seconds to achieve temperatures as low as 4 K (0.0004 eV).

ANTIHYDROGEN DETECTOR

Once antihydrogen is formed in the trap, it will no longer be contained by the electric and magnetic fields, and will move in a straight line out of the system. Once it collides with the electrode wall or with a background gas atom, both the positron and the antiproton will annihilate almost simultaneously, within about 1 ns of each other.

The antihydrogen detector will surround the vacuum system of the recombination trap. The detector detects the products of both the antiproton and the positron annihilations. The annihilation of antihydrogen is distinguished from that of unbound antiprotons and positrons by the fact that with antihydrogen both the antiproton and the positron annihilate at the same point in time and space.

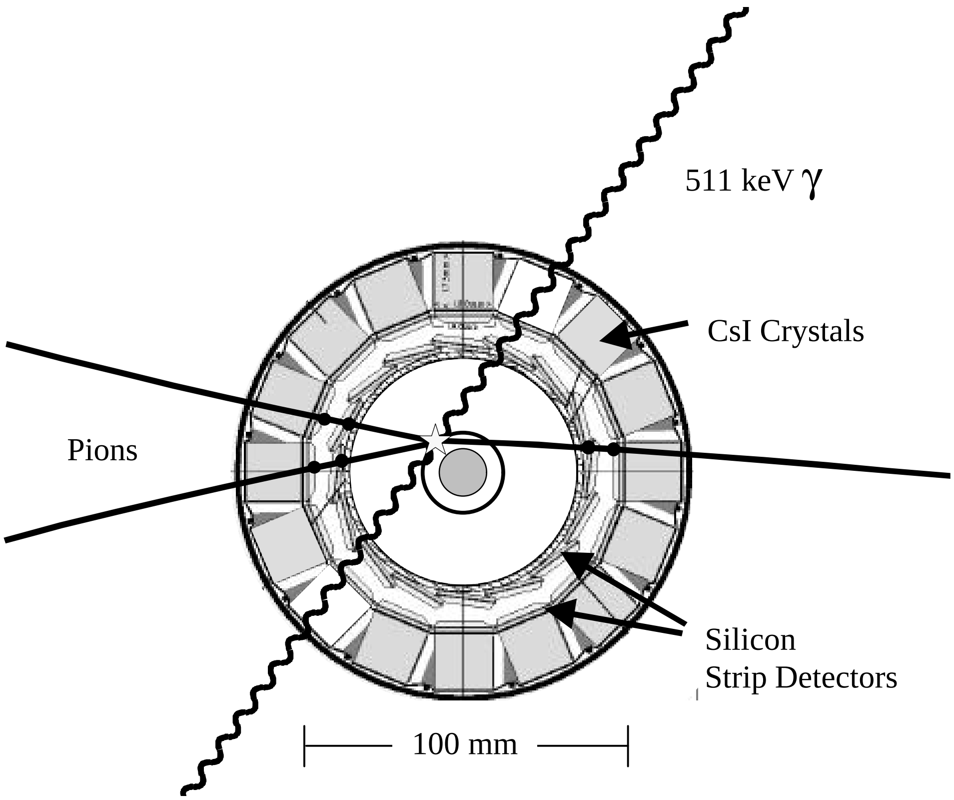

FIGURE 5: Cross section of the antihydrogen detector and recombination trap. The charged particles are in the center; the inner black ring represents the electrode where annihilation occurs. The 511 keV gammas are detected by the CsI crystals and the pions by the silicon strip detectors. Drawing is to scale.

The annihilation of an antiproton on a nucleon produces on average 3 to 4 charged pions in the 50 to 900 MeV energy range. Si strip detectors, arranged in two layers around the recombination trap, measure two points of the trajectories. Each layer of strip detectors consists of 16 detector modules arranged around the circumference, with each module having 128 strips on one side (r-φ) and 128 pads (z) on the other side. The vertex of the antiproton annihilation is determined by the intersection of the lines extrapolated from the measured points on the strip detectors. The error on the vertex position is largely dominated by the unknown curvature of the pion tracks, leading to an average extrapolation error of about 1 mm.

The annihilation of a positron produces two 511 keV back-to-back gamma rays. They are detected in an array of 16 (r) x 12 (φ) CsI crystals with dimensions 17 (r) x 17.5 (φ) x 13 (z) mm, surrounding the Si strip detectors. If two crystals register energy deposits compatible with 511 keV gamma rays within about 1 microsecond of an antiproton annihilation, it is assumed that they originate from within a straight line between the two crystals. For antihydrogen annihilation, it is then required that the vertex position determined by charged pions lies within the errors in determining this line.

The figure of merit of the detector is the ability to pinpoint the vertex of these annihilations in space and time. This detector will locate the vertex of the pions to σ_Z ~ 5 mm, and $\sigma_{r\varphi}$ ~ 1 mm. The vertex of the gamma rays is located to a tube of radius σ_T ~ 7 mm. The time resolution of the device will be about 1 μSec.

Many details have been left out of this simplified description. The evidence for the existence of $\overline{\mathrm{H}}$ will be statistical, since there are several background sources. The main source of the 511 keV background is positrons annihilating in the material outside the detector. These positrons stem from pair creation by π^0 decay gamma rays, which are emitted during the antiproton-nucleon annihilation.

REFERENCES

1. Gabrielse, G., *et al*., ATRAP Collaboration, "The Production and Study of Cold Antihydrogen", Proposal to the SPSC, CERN, SPSC 97-8/P306, March 1997.
2. For a recent review, see Holzscheiter, M.H. and Charlton, M., *Rep. Prog. Phys.* **62**, 1-60 (1999) and references therein.
3. Collier, M.J.T., Jørgensen, L.V., Meshkov, O.I., van der Werf, D.P. and Charlton, M., "Development and Testing of a Positron Accumulator for Antihydrogen Production," presented at the AIP Conference on Nonneutral Plasma Physics, Princeton, NJ, August 2-5, 1999.
4. Greaves, R. G., Tinkle, M. D. and Surko, C. M., *Phys. Plasmas* **1**, 1439 (1994).
5. Ordonez, C. A., *Phys. Plasmas* **4**, 2313-5 (1997).
6. Müller, A. and Wolf, A., *Hyperfine Interact.* **109,** 233-67 (1997).
7. Wolf, A., *Hyperfine Interact.* **76** 189-201 (1993).
8. Chen, F.F., *Introduction to Plasma Physics and Controlled Fusion*, New York: Plenum Press, 1984, ch. 1, p. 11.
9. Anderegg, F., Hollmann, E. M. and Driscoll, C. F., *Phys. Rev. Lett.* **81**, 4875-8 (1998).